Quantitation of the Effects of an Internal Proline Residue on Individual Hydrogen Bond Stabilities in an α-Helix: pH-Dependent Amide Exchange in Melittin and [Ala-14]Melittin

Christopher E. Dempsey‡

Biochemistry Department, Bristol University, School of Medical Sciences, Bristol BS8 1TD, U.K.

Received November 6, 1991; Revised Manuscript Received February 19, 1992

ABSTRACT: pH-Dependent amide exchange rates in methanol have been measured for 21 of the 25 exchangeable backbone amides of [Ala-14]melittin (P14A), a synthetic analogue of bee venom melittin having a Pro to Ala substitution at residue 14. P14A, like melittin, adopts an α-helical conformation in methanol. As previously found for melittin [Dempsey, C. E. (1988) *Biochemistry 27*, 6893], the exchange data could be fit to curves calculated assuming acid and base catalysis by solvent from which residue-specific values of k_H and k_{OMe}, the acid- and base-catalyzed exchange rate constants, respectively, were determined. From a comparison of k_{min} values, where k_{min} is the minimum exchange rate in the curve defining the amide exchange rate as a function of pH, with those previously obtained from melittin, the relative stabilities of individual helical hydrogen bonds in the two peptides were calculated in terms of equilibrium constants for hydrogen-bond-breaking backbone fluctuations. Replacement of P14 in melittin with Ala results in stabilization of amides in a central turn of helix by up to 36-fold ($\delta\Delta G_{Pro-Ala}$ = 9 kJ mol^{-1}) and elsewhere throughout the helix (residues 5–21) by 2–10-fold. These data indicate a cooperative effect of the Pro to Ala substitution on helix stability and allow a qualitative description of the fluctuational properties of the melittin and P14A helices in methanol. The effects of proline on the properties of the melittin helix are compared with previous theoretical and empirical studies on the effect of proline on the structure and stability of α-helices.

Despite its properties as a helix-breaking amino acid, proline is often found within known or putative membrane-spanning helices of membrane proteins (Brandl & Deber, 1986). Consistent with this observation, the effects of proline on helix structure are not completely disruptive; a conformational change in only the residue preceeding proline allows accommodation of proline in a distorted helix in which all helical hydrogen bonds (except the Pro$_n$ to X$_{n-4}$ hydrogen bond) can be formed (Piela et al., 1987). Helices can continue reasonably intact through a proline residue, and, in a nonpolar environment, isolated helices containing proline can be stable. On the other hand, proline-containing helices are distorted; analysis of helices in crystalline proteins has shown that helical segments N- and C-terminal to the proline are bent away from one another with bend angles usually around 20°, but in some cases as high as 50°. This bending reflects increased flexibility around the proline residue caused by the loss of at least one helical hydrogen bond. These structural constraints induced by proline have been investigated in several studies (Piela et al., 1987; Barlow & Thornton, 1988; Yun et al., 1991). The present paper describes the effects of proline on helix flexibility in an isolated helical peptide, melittin, determined by measuring the stability of individual helical hydrogen bonds using amide exchange analysis.

Melittin is a 26 amino acid peptide, containing a proline at residue 14, that hemolyzes erythrocytes at micromolar concentrations and induces voltage-dependent ion conductance in membranes at nanomolar concentrations (Habermann & Jentsch, 1967; Habermann, 1972; Tosteson & Tosteson, 1981; Hanke et al., 1983; Dempsey, 1990). Melittin adopts an amphipathic α-helical conformation in water at high concentrations (as a tetramer) (Terwilliger & Eisenberg, 1982), in methanol (Bazzo et al., 1988), in detergent micelles (Inakaki et al., 1989), and in membranes (Drake & Hider, 1979; Vogel, 1987). The proline-induced structural perturbation differs depending on the environment. In the aqueous tetramer, the N- and C-terminal helical segments are oriented at 50° to one another (Terwilliger & Eisenberg, 1981). The NMR-derived[1] structures of monomeric melittin in methanol (Bazzo et al., 1988) and in dodecylphosphocholine micelles (Inagaki et al., 1989) indicate that the angle between the N- and C-terminal helices, although not uniquely determined, may be only 20°. Amide exchange analysis of melittin in methanol indicates that P14 destabilizes hydrogen bonds in one turn of helix (involving the NHs of G12, L13, and A15), effectively separating the N- and C-terminal helical segments with a flexible helical bend (Dempsey, 1988).

To determine the effects of P14 on the stability of individual hydrogen bonds in the isolated melittin helix, we have prepared an analogue with a proline to alanine substitution at residue 14 ([Ala-14]melittin; P14A). P14A adopts an extended, stable, α-helical conformation in methanol without the flexible region around the proline residue found in melittin (Dempsey et al., 1991). The P14A analogue is considerably less effective than melittin in supporting voltage-dependent ion conductance in planar bilayers, an effect ascribed to the lack of flexibility in the center of the helix that allows alleviation of C-terminal charge repulsion in the transbilayer aggregates thought to underlie ion conductance (Dempsey et al., 1991). Here we describe an analysis of hydrogen exchange from individual amides of P14A and compare these data with similar data for melittin, allowing the effects of P14 on individual hydrogen bonds of the melittin α-helix to be quantitated in terms of equilibrium constants for backbone fluctuations that transiently

‡C.E.D. is a member of the Bristol University Centre for Molecular Recognition supported by the SERC.

[1] Abbrevations: NOESY, nuclear Overhauser enhancement spectroscopy; NMR, nuclear magnetic resonance; P14A, [Ala-14]melittin.

0006-2960/92/0431-4705$03.00/0

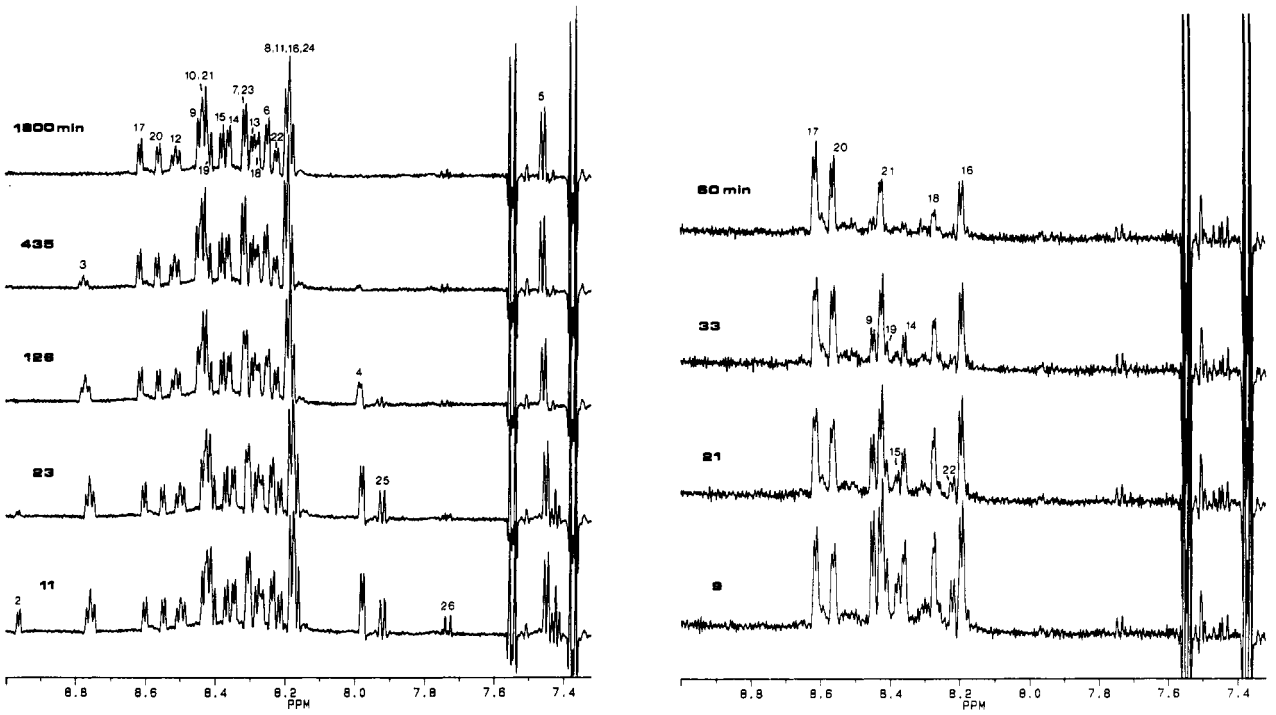

FIGURE 1: Amide region of 500-MHz ^{1}H NMR spectra of P14A (4 mM) at increasing times after dissolving in CD_3OD (24 °C) at pH* 1.8 (left) or pH* 6.8 (right).

break helical hydrogen bonds.

Materials and Methods

Melittin and P14A were prepared and purified to greater than 96% homogeneity as described (Dempsey & Sternberg, 1991). The assignments of the amide region of the ^{1}H NMR spectrum of P14A in methanol were described previously (Dempsey et al., 1991).

Time-resolved amide exchange experiments were done by following the loss of amide signal intensity in the ^{1}H NMR spectrum after dissolving the freeze-dried peptides in CD_3OD (Dempsey, 1988). Exchange experiments were done using the Bruker AM 500 or WH 300 spectrometers of the Oxford Centre for Molecular Sciences and the Jeol GSX 500 spectrometer of the Bristol University Centre for Molecular Recognition. NOESY spectra under conditions of partial amide exchange were obtained (at 28 °C) on the Jeol GSX 500 spectrometer using a mixing time of 350 ms. Exchange measurements were made at 24 °C, and the measured exchange rate constants were normalized to 20 °C by using activation energies for the exchange process determined by Englander et al. (1979). The peptide concentration was 3–5 mM. As found for melittin (Dempsey, 1988), there was no concentration dependence in the chemical shifts or exchange rates of amides in P14A at concentrations between 0.5 and 5 mM (not shown), indicating that self-association of the peptide is unlikely to occur in methanol over this concentration range.

pH* (the apparent pH) measurements in methanol were made with glass hydrogen combination electrodes (model CMAWL, Russell pH Electrodes, Auchtermuchty, Scotland) calibrated with aqueous buffers, and pH* readings from two different electrodes were averaged to give the pH* values quoted. The independent values were always within 0.2 pH units of one another. As described previously [see Dempsey (1988) for a detailed discussion], reliable pH-dependent amide exchange data can be obtained in methanol because the apparent pH (pH*) is a linear function of the true deuteron ion activity and because small changes in residual water content that greatly affect the difference between the true pH and pH* are apparently compensated by changes in the activities of the amide exchange catalysts (solvent D^+ and CD_3O^-).

pH-dependent exchange data were fitted by a least-squares algorithm to curves defined by eq 1 (Leichtling & Klotz,

$$k_{ex} = k_D[D^+] + k_{OMe}[OMe^-] + k_0 \quad (1)$$

1966), where k_{ex} is the experimental (pseudo) first-order exchange rate constant, k_D and k_{OMe} are the second order rate constants for acid- and base-catalyzed exchange, and k_0 is the first-order rate constant for pH-independent exchange. Base catalyst [OMe^-; see footnote 2 of Dempsey (1988)] concentrations were calculated with a value for the dissociation constant of methanol of $10^{-16.6}$ (Bates, 1973).

Results

Measurement and Analysis of Amide Exchange Rate Constants in P14A. The measurement of extensive exchange data was limited by the lack of dispersion of amide signals in the ^{1}H NMR spectrum of P14A (Figure 1) and by the stability of many of the amides to exchange at pH values near pH_{min} where exchange half-lives of many months at 24 °C were apparent. The analysis of pH-dependent amide exchange from melittin in methanol (Dempsey, 1988) showed that the exchange data could be fitted to eq 1 with k_0 equal to zero, and this was found also to be the case for the amides of P14A where exchange data over the complete pH-dependent exchange curves were accessible (Figure 3). From measurement of amide exchange in both the acid- and base-catalyzed limbs of the pH-dependent exchange curves sufficient to define k_D and k_{OMe} accurately, the value of pH^*_{min} and k_{min} (where pH^*_{min} is the pH*, and k_{min} the exchange rate constant, at the minimum of the pH-dependent exchange curves where $k_D[D^+] = k_{OMe}[OMe^-]$) can be calculated from eqs 2 and 3, respectively (Leichtling & Klotz, 1966):

$$pH^*_{min} = (1/2)[pK_{MeOD} - \log(k_{OMe}/k_D)] \quad (2)$$

$$k_{min} = k_D 10^{-pH_{min}} + k_{OMe} 10^{-(pK_{OMe} - pH_{min})} \quad (3)$$

Table I: Amide Exchange Parameters for Melittin P14A in Methanol at 20 °C

	k_D (min^{-1})	k_{OMe} (min^{-1})	pH*$_{min}$	k_{min} (min^{-1})	K_{op}
Ile-2	$5.82 \pm 1.38 \times 10^{-3}$	$2.78 \pm 0.55 \times 10^{13}$	0.45	4.03×10^{-3}	
Gly-3	$2.64 \pm 0.54 \times 10^{-2}$	$3.55 \pm 1.33 \times 10^{11}$	1.73	9.91×10^{-4}	
Ala-4	$1.48 \pm 0.31 \times 10^{-1}$	$1.31 \pm 0.48 \times 10^{11}$	2.33	1.65×10^{-3}	
Val-5	$1.02 \pm 0.24 \times 10^{-3}$	$6.50 \pm 1.26 \times 10^{9}$	1.89	2.65×10^{-5}	1.44×10^{-2}
Leu-6	$4.29 \pm 0.95 \times 10^{-4}$	$5.27 \pm 1.10 \times 10^{9}$	1.76	1.52×10^{-5}	8.59×10^{-3}
Lys-7	*	*	*	*	*
Val-8	$8.90 \pm 1.72 \times 10^{-4}$	$2.24 \pm 0.52 \times 10^{9}$	2.10	1.42×10^{-5}	8.02×10^{-3}
Leu-9	$6.91 \pm 1.98 \times 10^{-4}$	$7.97 \pm 1.31 \times 10^{8}$	2.27	7.45×10^{-6}	4.21×10^{-3}
Thr-10	*	*	*	*	*
Thr-11	$8.90 \pm 1.72 \times 10^{-4}$	$2.24 \pm 0.52 \times 10^{9}$	2.10	1.42×10^{-5}	8.02×10^{-3}
Gly-12	$2.59 \pm 0.45 \times 10^{-3}$	$4.22 \pm 0.58 \times 10^{9}$	2.19	3.67×10^{-5}	2.08×10^{-2}
Leu-13	$7.07 \pm 3.28 \times 10^{-4}$	$1.41 \pm 0.52 \times 10^{9}$	2.15	1.01×10^{-5}	5.71×10^{-3}
Ala-14	$8.06 \pm 2.65 \times 10^{-4}$	$8.52 \pm 1.73 \times 10^{8}$	2.28	8.21×10^{-6}	4.63×10^{-3}
Ala-15	$7.18 \pm 2.15 \times 10^{-4}$	$1.14 \pm 0.24 \times 10^{9}$	2.19	8.94×10^{-6}	5.05×10^{-3}
Leu-16	$2.75 \pm 0.13 \times 10^{-4}$	$2.06 \pm 0.84 \times 10^{8}$	2.37	2.39×10^{-6}	1.35×10^{-3}
Ile-17	$1.12 \pm 0.18 \times 10^{-4}$	$1.31 \pm 0.16 \times 10^{7}$	2.76	3.79×10^{-7}	2.14×10^{-4}
Ser-18	$2.07 \pm 0.53 \times 10^{-4}$	$2.30 \pm 0.41 \times 10^{8}$	2.27	2.47×10^{-6}	1.24×10^{-3}
Trp-19	$1.88 \pm 0.40 \times 10^{-4}$	$7.82 \pm 1.38 \times 10^{8}$	1.99	3.71×10^{-6}	2.09×10^{-3}
Ile-20	$1.18 \pm 0.26 \times 10^{-4}$	$3.90 \pm 0.43 \times 10^{7}$	2.55	6.85×10^{-7}	3.87×10^{-4}
Lys-21	$1.10 \pm 0.29 \times 10^{-3}$	$2.12 \pm 0.47 \times 10^{8}$	2.66	4.84×10^{-6}	2.73×10^{-3}
Arg-22	$1.59 \pm 0.49 \times 10^{-3}$	$8.42 \pm 1.74 \times 10^{8}$	2.43	1.11×10^{-5}	6.27×10^{-3}
Lys-23	*	*	*	*	*
Arg-24	*	*	*	*	•
Gln-25	$2.17 \pm 0.51 \times 10^{-1}$	$7.96 \pm 1.63 \times 10^{9}$	3.03	4.17×10^{-4}	2.36×10^{-1}
Gln-26	$9.33 \pm 2.19 \times 10^{-1}$	$4.89 \pm 1.08 \times 10^{9}$	3.44	6.78×10^{-4}	3.83×10^{-1}

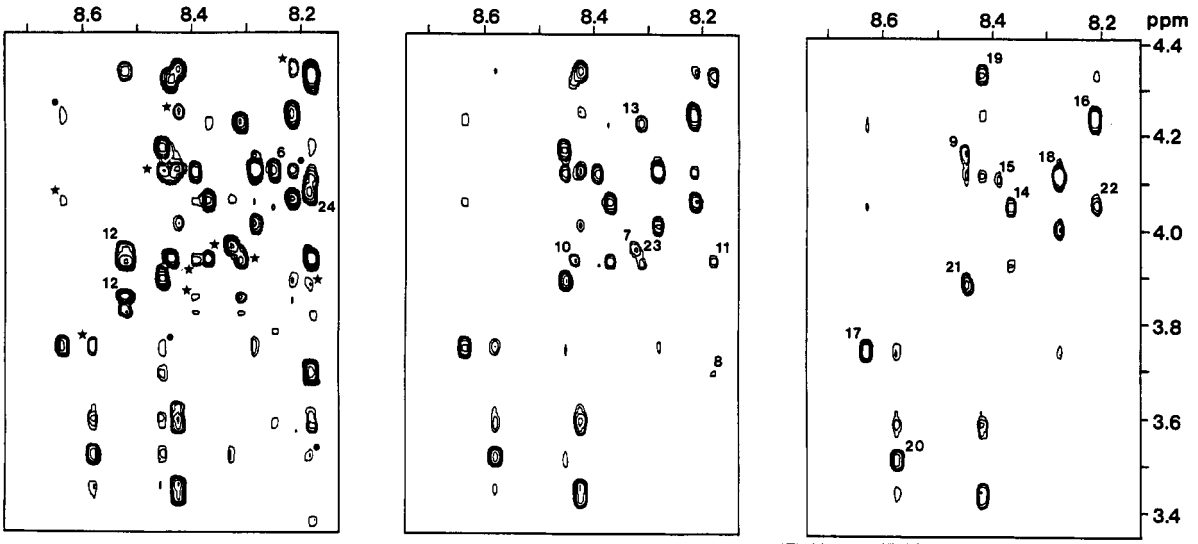

FIGURE 2: NHCHα region of NOESY spectra of P14A in CD_3OD (28 °C) at increasing times (6, 48, and 170 h, left to right) after being dissolved in CD_3OD at pH* 4.7. α_i–NH_i cross peaks are indicated by residue number in the panel in which the cross peak is last detectable. NOE's supporting α-helical structure [α_i–NH_{i+3} (●); α_i–NH_{i+4} (*)] are labeled in the first panel.

pH-dependent exchange data unaffected by spectral overlap were obtained for the amides of residues 2–6, 9, 12–15, 17–20, 22, and 25–26, and sufficient data were obtained to determine values for k_D and k_{OMe} to an accuracy of ±20%. Analysis of the multiexponential exchange curves for the overlapping signals centered around 8.18 ppm (the amides of 8, 11, 16, and 24) allowed good resolution of the two slowest rate constants differing by a factor of 5–8 depending on the pH. The slowest of these rates was assigned to L16, and the other was assigned to the amides of V8 and T11 (i.e., the amides of V8 and T11 are essentially unresolvable with rate constants at all values of pH differing by a factor of 3 or less). The exchange data for V8 and T11 in Table I and Figure 3 are an average of two values which, however, differ by only a small factor from each other. Likewise, the slowest exchange constant for the unresolved multiplets at 8.44 ppm (T10 and K21) was assigned to K21. These assignments were made from NOESY spectra obtained during exchange experiments; Figure 2 shows, for example, that K21 exchanges more slowly than T10 and that L16 exchanges more slowly than V8 and T11. Although exchange rates could be extracted from multiexponential curves for the other components of these multiplets (T10 and R24), the values did not fit well onto pH-dependent exchange curves and data for these amides are omitted. Likewise, the overlapping multiplets at 8.32 ppm (K7 and K23) gave a biexponential decay at all values of pH from which two exchange rate constants could be determined. There is no reliable basis for assigning these rate constants to the two amides, and so data for K7 and K23 are also omitted. It can be noted, however, that the log k_{min} value extracted from these data (taking either the average value or using either of the two independent values) is close to the k_{min} values for the amides of residues 6–9.

Fits of pH-dependent exchange data for the amides of P14A and comparison with similar data for melittin are shown in Figure 3, and the exchange parameters for all the amides of P14A are listed in Table I.

Equilibrium Constants for Hydrogen-Bond-Breaking Backbone Fluctuations. Exchange of hydrogen-bonded peptide amides is though to occur during backbone fluctuations

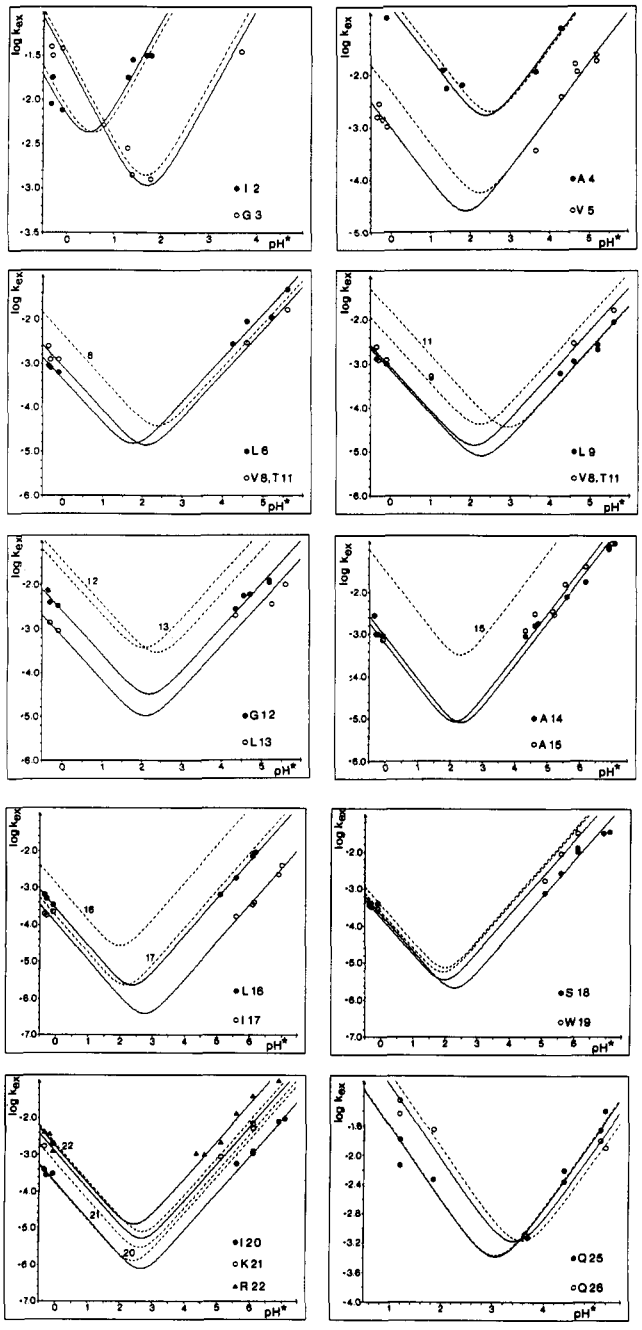

FIGURE 3: pH dependence of pseudo-first-order exchange rate constants of amides of P14A (solid curves) and melittin (broken curves) in CD_3OD normalized to 20 °C. The curves are least-squares fits to eq 1 with k_0 equal to zero. pH* values are direct meter readings using a hydrogen electrode calibrated with aqueous buffers. The curves for melittin amides are labeled with residue number except where they lie close to the exchange curve for the corresponding amide in P14A.

that transiently cleave hydrogen bonds (Englander & Kallenbach, 1984). The nature of these fluctuations is generally poorly defined both in extent and time scale, and there is evidence for exchange-limiting fluctuations encompassing global protein unfolding, cooperative fluctuations involving concerted opening of sequential hydrogen bonds of α-helices or β-sheets, or strictly local breaking of individual hydrogen bonds (Woodward et al., 1982; Wagner, 1983; Englander & Kallenbach, 1984; see Discussion). The fluctuations that limit amide exchange occur over a wide range of time scales but are much slower than the picosecond fluctuations of molecular dynamics simulations (Wagner, 1983). Without making any assumptions about the nature of the fluctuations other than the requirement for hydrogen-bond cleavage, the exchange

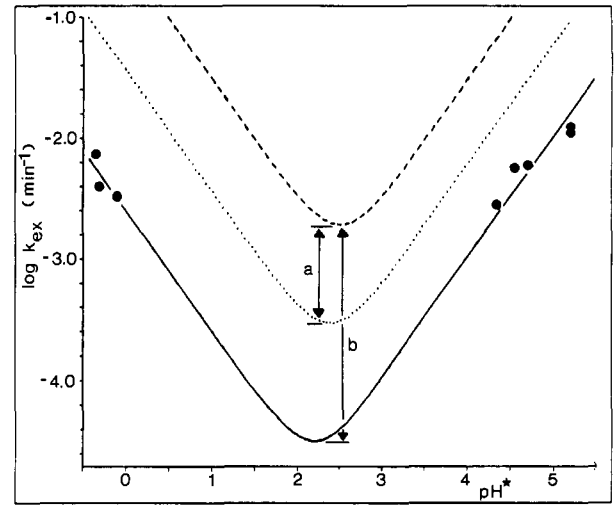

FIGURE 4: Illustration of the determination of $K_{op(P14A)}$ and $\delta K_{op(ML/P14A)}$ values listed in Tables I and II. Solid circles and curve are exchange data points and least-squares fit to eq 1 (with k_0 equal to zero), respectively, for exchange of G12 of P14A in CD_3OD at 20 °C. The dotted curve is the corresponding exchange curve for G12 of melittin, and the dashed curve is the exchange data for A4 NH which is not hydrogen-bonded (see text).

Table II: Comparison of Backbone Amide Stabilities in Melittin and Melittin-P14A

	$k_{min(ML)}$ (min^{-1})	$K_{op(ML)}$	$K_{op(P14A)}$	$\delta K_{op(ML/P14A)}$
Ile-2	4.28×10^{-3}			
Gly-3	1.42×10^{-3}			
Ala-4	1.89×10^{-3}			
Val-5	5.40×10^{-5}	3.05×10^{-2}	1.44×10^{-2}	2.12
Leu-6	*	*	8.59×10^{-3}	*
Lys-7	*	*	*	*
Val-8	3.84×10^{-5}	2.17×10^{-2}	8.02×10^{-3}	3.69
Leu-9	4.24×10^{-5}	2.40×10^{-2}	4.12×10^{-3}	5.70
Thr-10	6.26×10^{-5}	3.54×10^{-2}	*	*
Thr-11	3.67×10^{-5}	2.07×10^{-2}	8.02×10^{-3}	2.58
Gly-12	2.95×10^{-4}	1.46×10^{-1}	2.08×10^{-2}	7.01
Leu-13	3.50×10^{-4}	1.97×10^{-1}	5.71×10^{-3}	34.6
Ala-14			4.63×10^{-3}	*
Ala-15	3.20×10^{-4}	1.81×10^{-1}	5.05×10^{-3}	35.85
Leu-16	2.60×10^{-5}	1.46×10^{-2}	1.35×10^{-3}	10.81
Ile-17	2.41×10^{-6}	1.36×10^{-3}	2.14×10^{-4}	6.36
Ser-18	7.71×10^{-6}	4.36×10^{-3}	1.24×10^{-3}	3.52
Trp-19	5.78×10^{-6}	3.27×10^{-3}	2.09×10^{-3}	1.57
Ile-20	1.25×10^{-6}	7.06×10^{-4}	3.87×10^{-4}	1.82
Lys-21	3.90×10^{-6}	2.20×10^{-3}	2.73×10^{-3}	0.81
Arg-22	9.94×10^{-6}	5.62×10^{-3}	6.27×10^{-3}	0.90
Lys-23	2.96×10^{-5}	1.67×10^{-2}	*	*
Arg-24	1.01×10^{-4}	5.71×10^{-2}	*	*
Gln-25	4.26×10^{-4}	2.41×10^{-1}	2.36×10^{-1}	1.02
Gln-26	6.54×10^{-4}	3.96×10^{-1}	3.83×10^{-1}	0.96

process can be modeled in terms of transitions between hydrogen-bonded native (N) conformers and "open" (O) conformers from which the amide hydrogen can exchange with solvent (Hvidt & Neilsen, 1966):

$$N(H) \underset{k_2}{\overset{k_1}{\rightleftharpoons}} O(H) \xrightarrow{k_3} O(D) \underset{k_1}{\overset{k_2}{\rightleftharpoons}} N(D) \qquad (4)$$

Amide exchange from melittin (Dempsey, 1988) and P14A in methanol occurs in the EX_2 limit where the exchange-limiting fluctuation is in preequilibrium with chemical exchange ($k_2 \gg k_3$; Hvidt & Neilsen, 1966). In the EX_2 limit, the first-order exchange rate constant k_{ex} is given by

$$k_{ex} = (k_1/k_2)k_3 = K_{op}k_3 \qquad (5)$$

Values for K_{op}, the equilibrium constant characterizing the exchange-limiting backbone fluctuation, can be determined from values of k_{ex} if k_3 is known. While values for k_3 can be

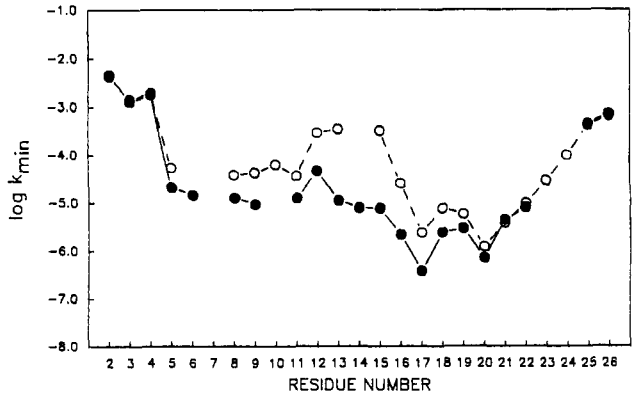

FIGURE 5: Log k_{min} values as a function of amino acid sequence for individual amides in P14A (●) and melittin (○) in CD_3OD at 20 °C.

estimated from the data of Molday et al. (1972), it is also possible to determine K_{op} directly as the ratio $k_{min(free)}/k_{min}$, where $k_{min(free)}$ is k_{min} for a non-hydrogen-bonded amide free to exchange with solvent (see Figure 4). This approach, which is used here, minimizes errors arising from uncertainties in the value of k_3 by including exchange contributions in both the acid- and base-catalyzed limbs of the exchange curves but contains the assumption that non-sequence-dependent (electrostatic) contributions to the stability of exchange intermediates have equal and opposite effects on the acid- and base-catalyzed exchange rate constants [see Dempsey (1988)]. An average value of k_{min} for the amides of G3 and A4 of melittin and P14A was used as $k_{min(free)}$ because these amides are not hydrogen-bonded (Bazzo et al., 1988). Table II lists values of K_{op} for the amides of P14A calculated as the ratio $k_{min}/k_{min(free)}$ (10^{-b} of Figure 4) and the ratios of the values of K_{op} for P14A and melittin, respectively (δK_{op}; $10^{(b-a)}$ of Figure 4).

Comparison of the k_{min} values of P14A and melittin as a function of amino acid sequence (Figure 5) shows that replacement of P14 with alanine considerably stabilizes amides in the central turn of helix (amides of residues 12–15 are stabilized by up to 36-fold). Amides in the N- and C-terminal helices up to seven or eight residues from the site of substitution are also stabilized by 2–6-fold. Thus, the presence of proline destabilizes amides to some extent throughout almost the entire helix. The sequential loss of stability of amides toward the C-terminus in melittin (Dempsey, 1988) is reproduced in P14A. The C-terminal helical section retains an overall increased stability relative to the N-terminal helical section previously observed in melittin.

Discussion

Effect of Proline-14 on Hydrogen Bond Stabilities in Melittin. Recent structural and theoretical analyses have detailed the structural consequences of an internal proline on an α-helix. Theoretical analysis has shown that proline can be accommodated in a distorted α-helix by a conformational change in only the residue X_{n-1} (where Pro is n) (Piela et al., 1987). Analysis of proline-containing helices in crystalline proteins demonstrates that proline induces a significant kink within helices where the kink angle (the angle of bisection of the axes of the helical segments N- and C-terminal to Pro_n) is usually around 26°. In the general case, the proline results in the loss of the P_n–X_{n-4} hydrogen bond (because of the absence of an amide hydrogen at Pro_n) and the X_{n+1}–X_{n-3} hydrogen bond where the N_{n+1}–O_{n-3} distance (~4.1 Å) is well above the acceptable limit for a hydrogen bond (Barlow & Thornton, 1988). Experimental studies of the effect of proline on the stability of isolated helices have not been made because of the marginal stability of helices in water. Analysis of free energy contributions to folding of dimerizing α-helical host peptides containing guest amino acids (O'Neill & DeGrado, 1990) showed that proline destabilized dimerization (and associated helix formation) by 14 kJ mol^{-1} ($\delta\Delta G$ Ala→Pro). Isolated helices containing proline are stabilized in solvents of low dielectric constant, allowing the effects of proline on helix stability within the folded state to be measured by analysis of the hydrogen exchange properties of hydrogen-bonded amides. This analysis differs from commonly used methods of determining free energy contributions of amino acid substitutions to protein stability where free energy differences between the folded state and temperature- or denaturant-induced unfolded states ($\delta\Delta G_u$) are measured. Amide exchange analysis allows local hydrogen-bond stabilities within the folded state to be measured in terms of equilibrium constants for the hydrogen-bond-breaking fluctuations of individual hydrogen bonds that limit amide exchange. These local free energies within the folded state differ from free energies of folding (they are smaller and the activation energies for the underlying structural fluctuations are lower), except in those cases where amide exchange is limited by total unfolding of the protein (Hilton et al., 1981; Wedin et al., 1982; Jandu et al., 1990).

In line with the observations described above, the helical hydrogen bond expected to be most perturbed by P14 is the A15N–T11O hydrogen bond (X_{n+1}–X_{n-3}). In melittin, however, a complete turn of helix involving the amides of residues G12, L13, and A15 is destabilized, and the substitution of P14 with A results in approximately equal stabilization of the amides of A15 (X_{n+1}–X_{n-3}) and L13 (X_{n-1}–X_{n-5}) by 35–36-fold (9 kJ/mol), indicating a cooperative effect of the P–A substitution on the stability of this pair of amides. G12 (X_{n-2}–X_{n-6}) is only stabilized by 7-fold relative to G12 of melittin; although in P14A this hydrogen bond is highly populated ($K_{op} \sim 2 \times 10^{-2}$), a local structural fluctuation allows this hydrogen bond to break more readily than other hydrogen bonds within the helix, an effect which may be peculiar to glycine in isolated α-helices as discussed in the following section.

To the extent that helical hydrogen bonds in methanol-solubilized melittin exhibit cooperative behavior, the substitution of P with A will stabilize other hydrogen bonds within the helix. This is observed in P14A throughout much of the helix from V5 (X_{n-9}) to I20 (X_{n+6}). Large stabilizations are observed for L16 NH (10-fold) and I17 NH (6-fold) even though these hydrogen bonds are already rather stable in melittin [K_{op} = 0.015 (L16); K_{op} = 0.0014 (I17)]. This enhanced stability of amides throughout the helix is characteristic of the cooperativity of hydrogen-bonded secondary structure.

Fluctuational Cooperativity in Melittin and P14A. The hydrogen-bond-breaking fluctuations that limit amide exchange from secondary structural units may involve concerted breaking of sequential hydrogen bonds or may be limited to individual or subclasses of hydrogen bonds. From equilibrium exchange data, it is straightforward to identify amides that do *not* share concerted hydrogen-bond-breaking fluctuations, because these amides have different values of K_{op}. Thus, in melittin, the N-terminal amides (of residues 5–11) must exchange through fluctuations that differ from those of the more stable C-terminal amides. Likewise, in P14A, the very stable amides at the C-terminal end of the helix must exchange through different fluctuations from those limiting exchange of the N-terminal amides. Although the presence of A14 stabilizes amides throughout the melittin helix, the amides are not stabilized to a single level, indicating that amide exchange is not limited by total helix unfolding (helix–coil fluctuations),

although it is possible that totally unfolded conformers contribute to exchange of the most stable amides (residues 17–20 of each peptide). The enhanced stabilities of the C-terminal ends of the helices of melittin and P14A probably result from stabilizing interactions of the positively charged amino acids of residues 21–24 with the C-terminal helix dipole.

The question of concertedness of exchange-limiting fluctuations of amides having similar values of K_{op} cannot be conclusively answered from equilibrium exchange data (EX_2 limit) although the marked similarity of K_{op} values in the N-terminal sections of the helices (residues 5–11 of melittin; residues 5–15 of P14A) is consistent with the concerted opening of hydrogen bonds. The destabilization of G12 NH relative to the other amides in the P14A N-terminal helix probably results from an additional local fluctuation in which the hydrogen bond involving the G12 amide transiently breaks without disrupting hydrogen bonds in the rest of the helix. An unresolved problem in the study of amide exchange from polypeptides is that of the minimal structural perturbation required for breaking of a hydrogen bond (of a helix or of other secondary structural units) that allows the amide to exchange with solvent. It is not clear, for example, whether amides can exchange individually from an isolated α-helix. The exchange data for P14A indicate that glycine may be able to undergo sufficient distortion to allow breaking of a helical hydrogen bond and rotation of the N–H group to an orientation where exchange with solvent deuterons is possible without destabilizing the hydrogen bonds around it. It is important to note that these considerations apply principly to isolated helices. In proteins, exchange from helices is likely to be less constrained by concerted helix fluctuations because of additional stabilizing interactions that may allow the transient distortions of helices required for nonconcerted hydrogen-bond-breaking fluctuations, and there are interpretations in the literature that support both concerted (Wand et al., 1986) and nonconcerted helix-opening fluctuations (Wagner et al., 1984). In this regard, we consider the analysis of the melittin helix in methanol to give *intrinsic* conformational and fluctuational properties in an environment of low dielectric. These intrinsic properties will be modulated by molecular interactions as observed in the crystalline tetramer (Terwilliger & Eisenberg, 1982); not surprisingly, the amide exchange properties of membrane-bound melittin and of the aqueous melittin tetramer differ from those of monomeric melittin in methanol (C.E.D. and G. Butler, unpublished results).

C-terminal helix tailing in melittin and P14A is essentially superimposable (Figure 5; Table II); in each case the amides of residues 21–26 show a monotonic 4-fold decrease in hydrogen-bond stability in the direction of the C-terminus, and the K_{op} values for these amides are essentially the same for melittin and P14A. This result is of interest because it indicates that the observed helix tailing is a function only of the position of these amides at the C-terminus and is independent of the stability of the internal section of the helix.

Amide Chemical Shifts. Of the characteristic proton NMR chemical shifts of proteins, the amide chemical shift is the most amenable to quantitative interpretation (Wagner et al., 1983); when contributions from ring current shifts are removed, the amide chemical shift correlates with hydrogen-bond length, with downfield shifts corresponding to shorter hydrogen bonds. Replacing P14 of melittin with A in P14A causes large changes in the amide chemical shifts of many of the amide protons (Dempsey et al., 1991). In each case the shift is downfield (Figure 6), corresponding to shorter hydrogen bonds in P14A. This is most marked for the amide of A15, which undergoes almost a 1 ppm shift downfield in P14A relative to melittin.

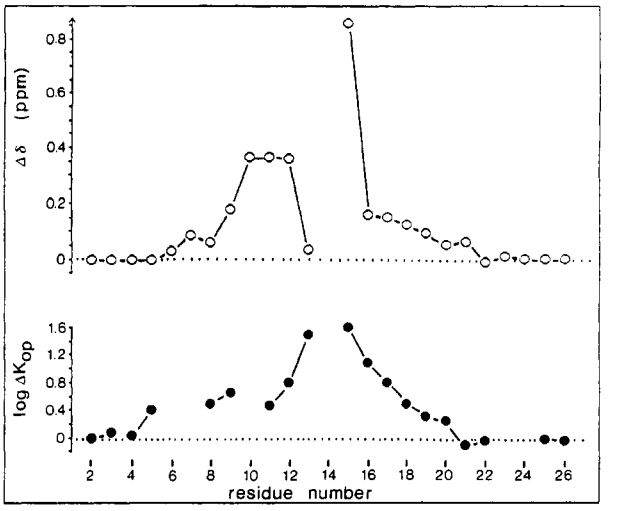

FIGURE 6: Comparison of the effect of substituting P14 of melittin with Ala on amide chemical shifts (○) and amide exchange stabilities (●) in CD_3OD. $\Delta\delta$ is the chemical shift of an amide in P14A minus the chemical shift of the corresponding amide of melittin; i.e., positive values are downfield shifts (indicating shorter hydrogen bonds; see text) in P14A relative to melittin. K_{op} values, calculated as indicated in Figure 4, are taken from Table II. Positive values of log ΔK_{op} indicate enhanced hydrogen-bond stabilities in P14A compared with melittin.

The major shifts are for those amides near the P14 residue, and the overall effect is a close juxtaposition of the chemical shifts of the amide signals in P14A (Figure 1). This is consistent with the formation of a regular helix in P14A with rather similar hydrogen-bond lengths throughout the region of stable helix. Amides in the helix termini (amides of residues 2–5 and 22–26) have the same chemical shifts in melittin and P14A. There is a qualitative correlation between the effect of the P14→A substitution on the amide chemical shift and the degree of stabilization of the hydrogen bond involving that amide (Figure 6). It might generally be expected that shorter hydrogen bonds correlate with greater hydrogen-bond stability [such correlations have been observed when comparing hydrogen-bond stabilities measured by amide exchange and hydrogen-bond fluctuations determined using molecular dynamics simulations (Levitt, 1981; Pastore et al., 1989)], but this will not always be the case. The length of a hydrogen bond is largely determined by the overall geometry of the secondary structural unit of which it is a part; in distorted secondary structure (like a bent helix; Blundell et al., 1983), some hydrogen bonds may be shorter while being part of a structure with high susceptibility to structure opening fluctuations. L13 NH with greatly enhanced stability to exchange in P14A compared with melittin has a negligible chemical shift change (Figure 6), and there are other examples of apparently shorter hydrogen bonds in mutant proteins where the amide hydrogen has an enhanced exchange rate [e.g., Gooley and MacKenzie (1990)].

Approaches to Determining Free Energies Using Amide Exchange. The use of amide exchange to measure free energy changes characterizing hydrogen-bond stabilities in native and mutated proteins requires an accurate measure of K_{op} values from exchange data. The approach used here takes into account the possibility that factors other than the primary effect on exchange (hydrogen bonding) and the commonly considered secondary factor (sequence-dependent inductive effects on the stabilities of exchange intermediates; Molday et al., 1972) affect amide exchange in polypeptides. The use of both acid- and base-catalyzed exchange rate constants in their combined effect on k_{min} is expected to correct for conformation-dependent electrostatic contributions that are known to affect amide

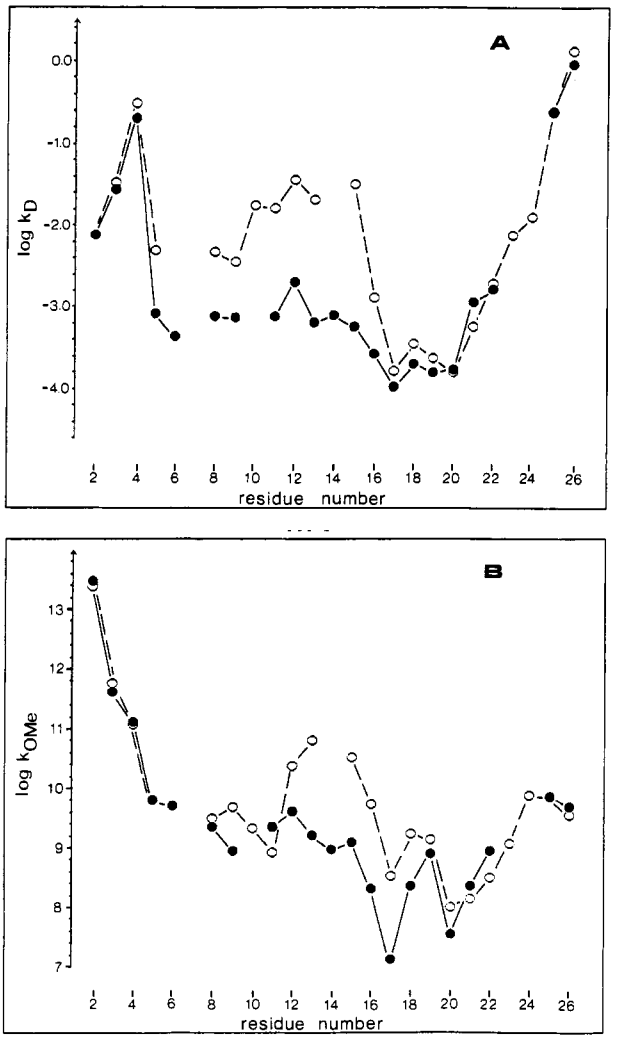

FIGURE 7: Logarithms of acid-catalyzed exchange rate constants (A) and base-catalyzed exchange rate constants (B) of P14A (●) and melittin (○) in CD_3OD (20 °C) as a function of amino acid sequence. The rate constants are not corrected for the sequence-dependent inductive contributions to exchange measured by Molday et al. (1972); these inductive contributions are identical for each peptide.

exchange in proteins because both the exchange catalysts (H^+ and OH^- or OMe^-) and the exchange transition states are charged (Englander & Kallenbach, 1984). In all studies for which experimental pH_{min} values have been compared with pH_{min} values calculated by incorporation of sequence-dependent inductive contributions, poor correlations are always observed (Tuchsen & Woodward, 1985a,b; Dempsey, 1986, 1988; Tuchsen & Woodward, 1987). These observations have been interpreted in terms of residual conformation-dependent contributions (global and local electrostatic effects and the accessibility of the amide carbonyl) in the transient "open" states from which exchange occurs. The combination of both acid- and base-catalyzed exchange rate constants is important when comparing exchange rates in nonpolar solvents (Dempsey, 1988) or micelles composed of charged detergents (O'Neil & Sykes, 1988) because electrode junction potentials or global charge effects can shift pH_{min} by several pH units. The use of k_{min} values for measuring equilibrium constants (K_{op}) contains its own implicit assumptions however (mainly the assumption that electrostatic effects have approximately equal and opposite effects on k_{acid} and k_{base}), and considering that generally in amide exchange studies of proteins extensive pH-dependent data are usually inaccessible, it is worth considering the two approaches.

If only the exchange protection factors measured in the base-catalyzed exchange regime are considered (Figure 7B), the amides stabilized by substituting Pro-14 of melittin for Ala in P14A segregate into the central and C-terminal part of the helix (amides of residues 12–20). Thus a consideration of exchange stabilities from base-catalyzed exchange rate constants gives a different picture from that obtained when k_{min} values are used to estimate K_{op}. Similarly, the acid-catalyzed exchange rate constants give large exchange slowing factors (P → A) for residues 5–16, i.e., they segregate into the N-terminal and central regions of the helix (Figure 7A). There is no available method that allows independent determination of K_{op} values for individual hydrogen bonds in hydrogen-bonded secondary structure, and it cannot be stated with certainty that the K_{op} values calculated from k_{min} are more accurate than values that would be calculated from the ratio of k_{OMe} (or k_D) for amides in melittin to k_{OMe} (or k_D) for the corresponding P14A amides. We know, as discussed above, that most (if not all) of the amides of melittin and P14A in methanol exchange from fluctuational intermediates in which helical structure is maintained to a greater or lesser extent. Any electrostatic contributions from actual or helix dipole charges in these partly structured transient states are expected to be at least approximately corrected for when combining acid- and base-catalyzed exchange rate constants in a measure of K_{op} values. In circumstances where hydrogen-bond fluctuations limiting amide exchange are associated with complete unfolding of the protein so that exchange occurs from conformations having the properties of a "random-coil" state, the use of base-catalyzed exchange rate constants to determine values of $\delta\Delta G$ when comparing the effects of single-site mutations on protein structural stability are likely to be accurate [e.g., Jandu et al. (1990)]. Where amide exchange occurs from states having residual conformation, residual conformation-dependent electrostatic contributions in the partially unfolded state from which exchange occurs might differ between the structural analogues of a protein. Such differential residual conformation-dependent effects between melittin and P14A probably underlie the enhancement of slowing factors in the acid-catalyzed regime for the N-terminal amide of P14A relative to melittin and the enhancement of base-catalyzed exchange slowing factors for the C-terminal amides (Figure 7). This might arise from an enhancement of helix dipole charges in the regular P14A helix over those in the melittin helix that would be expected to affect the stabilities of acid- and base-catalyzed exchange intermediates in the manner observed.

ACKNOWLEDGMENTS

I am grateful to Dr. R. Bazzo, who assigned the high-resolution proton NMR spectrum of P14A in methanol, to Dr. J. E. Fox for the excellent synthesis of P14A, and to Dr. I. D. Campbell for his interest in this work. The Oxford Centre for Molecular Sciences is acknowledged for use of the Bruker AM 500 spectrometer, and I thank Professor M. Green for access to the Bruker WH 300 spectrometer. I am particularly grateful to the Trustees of the Central Research Fund of Oxford University for financial support.

Registry No. Melittin, 37231-28-0; proline, 147-85-3.

REFERENCES

Barlow, D. J., & Thornton, J. M. (1988) *J. Mol. Biol. 201*, 601–619.

Bates, R. G. (1973) *Determination of pH: Theory and Practice*, Wiley, New York.

Bazzo, R., Tappin, M. J., Pastore, A., Harvey, T. S., Carver, J. A., & Campbell, I. D. (1988) *Eur. J. Biochem. 173*, 139–146.

Blundell, T., Barlow, D., Dorkakoti, N., & Thornton, J. (1983) *Nature (London) 306*, 281-283.
Brandl, C. J., & Deber, C. M. (1986) *Proc. Natl. Acad. Sci. U.S.A. 83*, 917-921.
Dempsey, C. E. (1986) *Biochemistry 25*, 3904-3911.
Dempsey, C. E. (1988) *Biochemistry 27*, 6893-6901.
Dempsey, C. E. (1990) *Biochim. Biophys. Acta 1031*, 143-161.
Dempsey, C. E., & Sternberg, B. (1991) *Biochim. Biophys. Acta 1061*, 175-184.
Dempsey, C. E., Bazzo, R., Harvey, T. S., Syperek, I., Boheim, G., & Campbell, I. D. (1991) *FEBS Lett. 281*, 240-244.
Drake, A. F., & Hider, R. C. (1979) *Biochim. Biophys. Acta 555*, 371-373.
Englander, J. J., Calhoun, D. B., & Englander, S. W. (1979) *Anal. Biochem. 92*, 517-524.
Englander, S. W., & Kallenbach, N. (1984) *Q. Rev. Biophys. 16*, 521-655.
Gooley, P. R., & MacKenzie, N. E. (1990) *FEBS Lett. 260*, 225-228.
Habermann, E. (1972) *Science 177*, 314-322.
Habermann, E., & Jentsch, J. (1967) *Hoppe-Seyler's Z. Physiol. Chem. 248*, 37-50.
Hanke, W., Metfessel, C., Wilmsen, H.-U., Katz, E., Jung, J., & Boheim, G. (1983) *Biochim. Biophys. Acta 727*, 108-114.
Hilton, B. D., Trudeau, K., & Woodward, C. K. (1981) *Biochemistry 20*, 4697-4703.
Hvidt, A., & Neilsen, S. O. (1966) *Adv. Protein Chem. 21*, 287-386.
Inagaki, F., Shimada, I., Kawaguchi, K., Hirano, M., Terasawa, I., Ikura, T., & Go, N. (1989) *Biochemistry 28*, 5985-5991.
Jandu, S. K., Ray, S., Brooks, L., & Leatherbarrow, R. J. (1990) *Biochemistry 29*, 6264-6269.
Leichtling, B., & Klotz, I. (1966) *Biochemistry 5*, 4026-4037.
Levitt, M. (1981) *Nature (London) 294*, 379-380.
Molday, R. S., Englander, W. S., & Kallen, R. G. (1972) *Biochemistry 11*, 150-158.
O'Neil, J. D. J., & Sykes, B. D. (1988) *Biochemistry 28*, 699-707.
O'Neill, K., & DeGrado, W. L. (1990) *Science 250*, 646-651.
Pastore, A., Harvey, T. S., Dempsey, C. E., & Campbell, I. D. (1989) *Eur. Biophys. J. 16*, 363-367.
Piela, L., Nemethy, G., & Scheraga, H. A. (1987) *Biopolymers 26*, 1587-1600.
Terwilliger, T. C., & Eisenberg, D. (1982) *J. Biol. Chem. 257*, 6016-6022.
Tosteson, M. T., & Tosteson, D. C. (1981) *Biophys. J. 36*, 109-116.
Tuchsen, E., & Woodward, C. (1985a) *J. Mol. Biol. 185*, 405-419.
Tuchsen, E., & Woodward, C. (1985b) *J. Mol. Biol. 185*, 421-430.
Tuchsen, E., & Woodward, C. (1987) *J. Mol. Biol. 193*, 793-802.
Vogel, H. (1987) *Biochemistry 26*, 4562-4572.
Wagner, G. (1983) *Q. Rev. Biophys. 16*, 1-57.
Wagner, G., Pardi, A., & Wüthrich, K. (1983) *J. Am. Chem. Soc. 105*, 5948-5949.
Wagner, G., Stassinopoulou, C. I., & Wüthrich, K. (1984) *Eur. J. Biochem. 145*, 431-436.
Wand, A. J., Roder, H., & Englander, S. W. (1986) *Biochemistry 25*, 1107-1114.
Wedin, R. E., Delepierre, M., Dobson, C. M., & Poulsen, F. M. (1982) *Biochemistry 21*, 1098-1103.
Woodward, C. K., Simon, I., & Tuchsen, E. (1982) *Mol. Cell. Biochem. 48*, 135-160.
Yun, R. H., Anderson, A., & Hermans, J. (1991) *Proteins 10*, 219-228.

Conformational Properties of B-Z Junctions in DNA†

Min Lu,‡ Qiu Guo, and Neville R. Kallenbach
Department of Chemistry, New York University, New York, New York 10003
Richard D. Sheardy*
Department of Chemistry, Seton Hall University, South Orange, New Jersey 07079
Received November 21, 1991; Revised Manuscript Received March 10, 1992

ABSTRACT: The structural consequences of specific base sequences in DNA can exert a strong influence on the function of DNA. It has previously been reported that the presence of multiple B-Z conformational junctions in constructed DNA oligomers results in unusually *enhanced* electrophoretic gel mobilities of these oligomers [Winkle, S. A., & Sheardy, R. D. (1990) *Biochemistry 29*, 6514-6521]. In order to investigate this phenomenon further, we designed and synthesized several DNA oligomers capable of pure Z or B-Z junction formation for polyacrylamide gel electrophoresis studies. The results indicate that both pure Z-DNA and polymorphic B-Z-DNA oligomers exhibit unusual gel migratory properties. The results of gel mobility studies in the absence and presence of cobalt hexamine indicate that a B-Z junction corresponds to a stiff bend of the helix axis, with two or more conformers accessible at the junction site. This is a different bend and mechanism than that in oligo(A) tracts.

The conformation and dynamical properties of a segment of DNA are strongly dependent upon both its sequence and its environment. One approach to the study of sequence and environmental influences on the biophysical properties of nucleic acids is through rational design of model systems based upon short (i.e., 16-80 bp) DNA oligomers. Many unusual DNA structures have been revealed in this way, including left-handed conformations (Wang et al., 1979; Gessner et al., 1985), bent DNA (Wu & Crothers, 1984; Hagerman, 1984, 1985, 1986), branched DNA structures (Ma et al., 1986;

† This work was supported by Grant CA-24101 (N.R.K.) from the National Institutes of Health and Grant DMB-8996232 (R.D.S.) from the National Science Foundation.
* Author to whom correspondence should be addressed.
‡ Present address: Department of Biochemistry and Molecular Biology, Harvard University, Cambridge, MA 02138.

0006-2960/92/0431-4712$03.00/0